J. Math. Biol.
DOI 10.1007/s00285-012-0640-8

**Mathematical Biology**

# Dynamic spatial pattern formation in the sea urchin embryo

**Syed Shahed Riaz · Michael C. Mackey**

Received: 7 March 2012 / Revised: 16 December 2012


**Abstract** The spatiotemporal evolution of various proteins during the endo-mesodermal specification of the sea urchin embryo in the form of an expanding torus has been known experimentally for some time, and the regulatory network that controls this dynamic evolution of gene expression has been recently partially clarified. In this paper we construct a relatively simple mathematical model of this process that retains the basic features of the gene network and is able to reproduce the spatiotemporal patterns observed experimentally. We show here that a mathematical model based only on the gene-protein interactions so far reported in the literature predicts the origin of the behaviour to lie on a delayed negative feed-back loop due to the protein Blimp1 on the transcription of its corresponding mRNA. However though consistent with earlier results, this contradicts recent findings, where it has been established that the dynamical evolution of Wnt8 protein is independent of Blimp1. This leads us to offer a modified version of the original model based on observations in similar systems, and some more recent work in the sea urchin, assuming the existence of a mechanism involving inhibitory loop on *wnt8* transcription. This hypothesis leads to a better match with the experimental results and suggests that the possibility of the existence of such an interaction in the sea urchin should be explored.

**Electronic supplementary material** The online version of this article (doi:10.1007/s00285-012-0640-8) contains supplementary material, which is available to authorized users.

S. S. Riaz (✉)
Department of Physiology, Centre for Applied Mathematics in Bioscience and Medicine, McGill University, 3655 Promenade Sir William Osler, Montreal, QC H3G 1Y6, Canada
e-mail: shahedrz@gmail.com

M. C. Mackey
Departments of Physiology, Physics and Mathematics,
Centre for Applied Mathematics in Bioscience and Medicine, McGill University,
3655 Promenade Sir William Osler, Montreal, QC H3G 1Y6, Canada
e-mail: mackey@cnd.mcgill.ca

Published online: 25 January 2013

**Keywords** Gene network · Oscillation · Traveling wave · Delayed feedback

## 1 Introduction

The developmental process in a living organism is controlled by the sequential expressions of a series of genes (Adimy et al. 2006). This sequential expression of genes in turn is governed by the developmental gene regulatory network (GRN) which precisely describes the interactions between transcription factors and cis-regulatory modules that control the expression of genes required for the developmental process. Therefore the genomic code that controls interactions that lead to the specification of embryonic territories, and its subsequent subdivision and differentiation, is largely governed by the GRN (Davidson 2006).

In this context the sea urchin embryo presents an interesting case study (Smith and Davidson 2008). Most of the key elements present in the genetic regulatory network of the sea urchin embryo have already been identified with their roles in the network known. This allows us to look for an overall understanding of how development works in this system as has recently been illustrated for the network that determines specification and differentiation of the skeletogenic micromere lineages or skeletogenic mesoderm (SM) of this embryo. In this paper we concentrate on another striking feature of the endo-mesodermal specification, viz. the concentrically expanding progression of *notch* and *wnt* signaling which, after being initiated in the SM, sweeps outward across the vegetal domains of the embryo.

Recent studies on the sea urchin embryo have claimed to reveal the entire sequence of regulatory gene activity in the vegetal domains of the embryo that entrains a set of genes in an expanding torus-like pattern of gene expression. Smith et al. (2007) showed that the regulatory circuitry underlying this phenomenon is a double feedback loop linking the *wnt8* and the *blimp1* regulatory genes. (The reader may find reference to Fig. 1 useful in following this discussion). cis-Regulatory studies show that the *wnt* genes require input from both $\beta$-catenine–Tcf and from Blimp1 protein for expression. Conversely, *blimp1* requires input from the same *wnt8/Tcf* signaling system as well as from another ubiquitous protein Otx (Minokawa et al. 2005; Davidson 2002). However, the *blimp1* gene also contains auto-repression sites which, after some hours when the Blimp1 protein attains a sufficiently high concentration, shuts down its own expression, and therefore that of *wnt8* as well (Livi and Davidson 2006). In the meantime Wnt8 has diffused outward to the next ring of cells and activated the feedback circuit there. The consequence is that following their initial expression in the centrally located SM territory, expression of these genes disappears from the SM and is activated in the non-skeletogenic micromere (NSM). However, after a few hours these genes are inactivated in the NSM and becomes activated in the next outer rings of prospective endoderm cells, producing an expanding torus-like pattern of gene expression. However it has been recently reported that although mutation of Blimp1-binding sites lowers the activity of a small *wnt8* cis-regulatory construct18, this does not affect expression of a bacterial artificial chromosome expression construct containing the whole genomic *wnt8* cis-regulatory system (Peter and Davidson 2011). Also it is always seen that the expression of

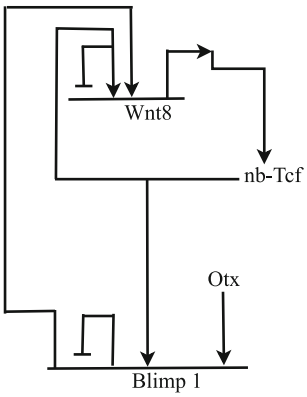


**Fig. 1** The gene regulatory network corresponding to the *wnt*8–*blimp*1 sub circuit. The *lines* with *arrowheads* denote activation and the ones with *blunt heads* denote inhibition

*wnt8* starts in veg2-derived cells long before the initiation of *blimp1b* expression in these cells. More over a recent publication suggests Notch protein may be in some way involved in the clearance of Wnt8 from the mesodermal domain during endo-mesodermal specification (Sethi et al. 2012). This might be indicative of the presence of some other feedback loop responsible for the clearance of Wnt8 from the SM.

Thus this system presents an interesting example of dynamic pattern formation due to a coupling between activator–inhibitor kinetics and diffusion. In the following sections we propose two variations of a same general model. One suggests the phenomena can be looked at as a delay induced propagation of traveling wave while the other interprets it in terms of local structure formation and its consequent effect on the immediate neighborhood. Our approach in the present paper is to start with a mathematical model for the temporal behavior of this process based on the simplest form of the architecture of the gene network that incorporates all of the essential experimental findings, and then to look at the spatio-temporal behavior when diffusive effects are taken into account.

The outline of the paper is as follows. In Sect. 2 we develop the full mathematical model based entirely upon the gene regulatory circuitry reported in the literature (Smith et al. 2007). Following some general remarks in Sect. 2.1 we turn to a development of the temporal evolution equations for the $blimp1$–$wnt8$ in Sect. 2.2.

Due to the relative complexity of the model there are a number of parameters, and in Sect. 2.3 we minimize their number by scaling. The estimation of the remaining parameters is given in Appendix A. Section 3 presents the numerical results, first for the temporal behavior alone in Sect. 3.1 and then for the full spatio-temporal behavior in Sect. 3.2. Because of the uncertainty of many of the parameters, in Sect. 3.3 we have carried out a sensitivity analysis. The analysis reveals that the auto inhibitory feed back loop due to Blimp1 protein on the transcription of corresponding mRNA is crucial for generating the instability required for the basic phenomena of evolution of proteins from the center. This matches well with the initial experimental finding which suggests Blimp1 protein has a pivotal role in Wnt8 evolution and subsequent clearance (Smith et al. 2007). But a later study (Peter and Davidson 2011) refutes this earlier

proposal and shows that the clearance of *blimp1* expression from the mesodermal domain may not be essential for the clearance of *wnt8* expression from the same region. This leads us to a qualitative modification of the original model in Sect. 4 where we have assumed a negative feedback loop involving Wnt8 protein and its mRNA. This assumption is based on observations in similar systems (Meinhardt 2012) and if verified experimentally could be of help in elucidating the exact mechanism by which Wnt8 works in many other biochemical pathways. A possible variation of this negative feed back loop involving *notch* signaling too has been explored. This is motivated by a very recent revelation regarding the role of Notch in the clearance of Wnt8 from the mesodermal domain (Sethi et al. 2012). The paper concludes in Sect. 5 where we discuss in detail how recent experimental observations in the sea urchin embryo forces us to modify our modeling approach and go beyond the existing regulatory network.

## 2 Model

A recent paper (Smith et al. 2007) summarizes the results of various experimental studies in the sea urchin embryo and proposes a complex regulatory network for the expression pattern of the genes during endo-mesodermal specification (Fig. 1).

### 2.1 General modeling comments

Below we present a mathematical model based on this architecture in order to understand the spatio-temporal dynamics of gene expression observed experimentally.

In the formulation of our model equations, transcription of *blimp1* gene to the corresponding mRNA is positively regulated by the proteins Wnt8 and Otx, and the transcription of *wnt8* gene to *wnt* mRNA is activated by Blimp1 protein. In addition, Blimp1 protein represses its own expression (i.e. the expression of *blimp1* mRNA from *blimp1* gene). The system consisting of *blimp1* and *wnt8* is thus self contained.

We model the inhibitory and the activation feedback terms by Hill functions (Santillan 2008) so that the feedback experienced by mRNA $P$ from protein $Q$ is given by

$$\begin{aligned} G_{PQ}(X) &= \frac{X^{n_{PQ}}}{k_{PQ}^{n_{PQ}} + X^{n_{PQ}}} \\ &\text{or} \\ F_{PQ}(X) &= \frac{k^{n_{PQ}}}{k_{PQ}^{n_{PQ}} + X^{n_{PQ}}}, \end{aligned} \tag{1}$$

depending upon whether the interaction is activated or inhibited by the controlling molecule $X$.

The translational rates are taken to be linearly related to the concentration of the corresponding mRNA. Further we assume random degradation for all the mRNAs and proteins. Finally we assume each of the transcription and the translation processes involve characteristic constant average delays. The delays arise in transcription because the polymerase takes a finite time to transcribe the genes. In the case of the translation

process the delay is due to the sum of the time required for movement of the mRNA to the cytosol and the time for its translation. For any variable $z$ the notation $z_\tau \equiv z(t-\tau)$ will be used whenever the variable is delayed, where $t$ denotes time.

In terms of diffusion effects, we assume that mRNA cannot diffuse between cells. Furthermore, the only protein capable of diffusing between cells is Wnt8 and thus a diffusion term must be included for this factor. When considering the spatial effects due to diffusion, $\chi$ will denote the spatial independent variable (unscaled).

Throughout the paper we denote a protein $X$ by $pX$ while an mRNA $X$ is denoted by $mX$.

### 2.2 The *blimp*1–*wnt*8 circuit

We focus on the dynamics of the regulation of the *blimp*1–*wnt*8 module in accordance with the network given in Fig. 1.

The *blimp*1 mRNA is denoted by $mB$ and the Blimp1 protein by $pB$. $pCt$ denotes the concentration of the complex formed between $\beta$-*catenin* and $TcSf$ The dynamics of $mB$ are described by the differential delay equation

$$\frac{dmB}{dt} = \kappa_{mB}\{[G_{BW}(pCt) + G_{BO}(pO)]F_{BB}(pB)\}_{\tau_{mB}} - \gamma_{mB}mB. \tag{2}$$

The first term reflects the increase in $mB$ due to the positive feedback effects of the $\beta$-*catenin*–$Tcsf$ complex as well as protein $Otx$ ($pO$), and the negative feedback effect of the Blimp1 protein on the production of the *blimp*1 mRNA. These effects occur with a delay $\tau_{mB}$ due to the time required for transcription of the DNA. The last term simply reflects the degradation of *blimp*1 mRNA. The dynamics of the Blimp1 protein are described by

$$\frac{dpB}{dt} = \kappa_{pB}\,[mB]_{\tau_{pB}} - \gamma_{pB}\,pB, \tag{3}$$

reflecting the assumption that the rate of production of $pB$ is simply proportional to the level of $mB$ at a time $\tau_{pB}$ in the past, where $\tau_{pB}$ is the time required for translation of the *blimp*1 mRNA, and that there is a concomitant degradation of the protein.

*Remark 1* Whether the two regulatory inputs will be additive or multiplicative depends on the molecular details of the interaction. Lacking such definite information we instead checked and made sure that our qualitative results do not depend upon any particular choice, and indeed our conclusions are the same even if we assume all the activating and inhibitory inputs appear in a multiplicative or additive fashion. In the text we described the case where two activating inputs are multiplicative while one activating and a second inhibitory one are additive. The important issue from the point of view of the qualitative dynamics is that the overall response of the combination to different inputs must have the same qualitative form regardless of whether inputs are additive or multiplicative.

In describing the dynamics of the $wnt8$ mRNA (denoted by $mW$) we have a similar equation

$$\frac{dmW}{dt} = \kappa_{mW}\left[G_{WB}\left(pB\right) + G_{WW}\left(pCt\right)\right]_{\tau_{mW}} - \gamma_{mW} mW, \tag{4}$$

reflecting the positive feedback exercised through both Blimp1 and $\beta$-catenin–Tcsf complex, again delayed due to the transcription delay $\tau_{mW}$ required to produce $mW$, and a degradation of $mW$. As for the Blimp1 protein, we assume the dynamics of the Wnt8 protein are determined by

$$\frac{\partial pW}{\partial t} = \kappa_{pW}\left[mW\right]_{\tau_{pW}} - \gamma_{pW} pW + D_{pW}\frac{\partial^2 pW}{\partial \chi^2}, \tag{5}$$

$\tau_{pW}$ is the translation time and there is linear degradation of the Wnt8 protein. $D_{pW}$ is the corresponding diffusion coefficient.

The dynamics of the nuclearization process can be expressed as

$$\frac{dpC}{dt} = \kappa_{pC} G_{wC}(pW) - \gamma_{pC} pC. \tag{6}$$

The first term on the right hand side of this equation represents the activation due to protein $pW$ which is assumed to follow Hill kinetics. $\beta$-catenin then functions as co-activator with Tcsf (tcf). We assume that this involves a fast equilibrium process and therefore the concentration of the complex pCt is proportional to both pC and tcf SO

$$pCt = K_{eq} \cdot pC \cdot tcf. \tag{7}$$

### 2.3 Reduction of parameters and their estimation

The model formulated in Eqs. 2–7 of the previous section consists of six evolution equations with numerous non-linearities and many parameters. Apart from the transcriptional and translational delays, there are four categories of parameters in the model: the degradation rates, the kinetic rate constants, the diffusion coefficient, and the Hill exponents. Identities of all the variables and parameters could be found in the Tables 1, 2 and 3. Ideally all the parameters in the model should be taken from the biochemical literature. Then we could ask what behavior the model shows, and thereby judge the degree to which it mimics the experimental results.

Unfortunately due to the lack of sufficient experimental data regarding the mRNAs and proteins involved in the network, this approach is not feasible for the model. Indeed, the estimation of all of these parameters would be a formidable task, if not impossible. Consequently we have eliminated as many of these parameters as possible through a judicious scaling of the equations.

We let $mb$, $mw$ denote dimensionless concentrations of the mRNAs for $blimp1$ and $wnt8$ respectively, and $pb$, $pw$ their corresponding proteins. There is no unique

**Table 1** This details the scaling that we have carried out on our model equations

| mRNA | Protein | Hill parameters |
|---|---|---|
| $mb = \frac{\gamma_{mB}}{\kappa_{mB}} mB$ | $pb = \frac{\gamma_{pB}\gamma_{mB}}{\kappa_{pB}\kappa_{mB}} pB$ | $k_{bw} = \frac{\gamma_{pB}\gamma_{mB}}{\kappa_{pB}\kappa_{mB}} K_{BW}, k_{bo} = \frac{\gamma_{pO}\gamma_{mO}}{\kappa_{pO}\kappa_{mO}} K_{BO}, k_{bb} = \frac{\gamma_{pB}\gamma_{mB}}{\kappa_{pB}\kappa_{mB}} K_{BB}$ |
| $mw = \frac{\gamma_{mW}}{\kappa_{mW}} mW$ | $pw = \frac{\gamma_{pW}\gamma_{mW}}{\kappa_{pW}\kappa_{mW}} pW$ | $k_{wb} = \frac{\gamma_{pB}\gamma_{mB}}{\kappa_{pB}\kappa_{mB}} K_{WB}, k_{ww} = \frac{\gamma_{pW}\gamma_{mW}}{\kappa_{pW}\kappa_{mW}} K_{WW}$ |
| $md = \frac{\gamma_{pD}}{\kappa_{mD}} mD$ | $pd = \frac{\gamma_{mD}\gamma_{mD}}{\kappa_{pD}\kappa_{mD}} pD$ | $k_{dr} = \frac{\gamma_{pR}\gamma_{mR}}{\kappa_{pR}\kappa_{mR}} K_{DR}, k_{dh} = \frac{\gamma_{pH}\gamma_{mH}}{\kappa_{pH}\kappa_{mH}} K_{DH}$ |
| - | $pc = \frac{\gamma_{mC}}{\kappa_{pC}} pC$ | $k_{cw} = \frac{\gamma_{pC}}{K_{pC}}$ |
| $mn = \frac{\gamma_{mN}}{\kappa_{mN}} mN$ | $pn = \frac{\gamma_{pN}\gamma_{mN}}{\kappa_{pN}\kappa_{mN}} pN$ | $k_{nu} = \frac{\gamma_{pU}\gamma_{mU}}{\kappa_{pU}\kappa_{mU}} K_{NU}, k_{nb} = \frac{\gamma_{pB}\gamma_{mB}}{\kappa_{pB}\kappa_{mB}} K_{NB}$ |
| $mh = \frac{\gamma_{mH}}{\kappa_{mH}} mH$ | $ph = \frac{\gamma_{pH}\gamma_{mH}}{\kappa_{pH}\kappa_{mH}} pH$ | $k_{hu} = \frac{\gamma_{pU}\gamma_{mU}}{\kappa_{pU}\kappa_{mU}} K_{HU}, k_{hni} = \frac{\gamma_{pD}\gamma_{mD}\gamma_{pN}\gamma_{mN}}{\kappa_{pD}\kappa_{mD}\kappa_{pN}\kappa_{mN}.K_{eq}} K_{hni}$ |
| | $pc = \frac{\gamma_{pC}}{\kappa_{pC}} pC$ | $k_{cw} = \frac{\gamma_{pW}\gamma_{mW}}{\kappa_{pW}\kappa_{mW}} K_{CW}$ |
| | $pct = \frac{\gamma_{pC}}{k_{pC}} pCt$ | |
| | $tcf = K_{eq} Tcf$ | |

Further we introduce dimensionless space coordinates $x = \chi/l$, and the scaled diffusion coefficient (of the $q$th species) $d_q = D_q/l^2$ (with $l$ having units of mm). It follows from these definitions that all of the variables and the parameters, except the degradation rates, time delays and the diffusion coefficients, are dimensionless. The degradation rates and diffusion coefficients have units of $\text{min}^{-1}$ and the time delays are expressed in min

**Table 2** Identities of the variables (in the dimensionless form) that are used throughout the paper

| | |
|---|---|
| $pw, pb, pn\ pc$ | Concentrations of proteins: Wnt8, Blimp1 and Notch and $\beta$-catenin |
| $mw, mb, mn$ | Concentrations of mRNAs: Wnt8, Blimp1 and Notch |
| $tcsf$ | Concentration of $beta$-catenin–tcsf complex |

**Table 3** Identities of the parameters used throughout the paper

| | |
|---|---|
| $\tau_{mb}, \tau_{mw}$ | Transcriptional time delay (in min) |
| $\tau_{pb}, \tau_{pw}$ | Translational time delay (in min) |
| $\gamma_{mb}, \gamma_{mw}$ | Degradation constants for mRNAs (in $\text{min}^{-1}$) |
| $\gamma_{pb}, \gamma_{pw}, \gamma_{pc}, \gamma_{pn}$ | Degradation constants for proteins (in $\text{min}^{-1}$) |
| $k_{bc}, k_{bb}, k_{wb}, k_{ww}, k_{wc}, k_{cw}, k_{bw}$ | Hill rate constants |
| $n_{bc}, n_{bb}, n_{wb}, n_{ww}, n_{wc}, n_{cw}, n_{bw}$ | Hill coefficients |
| $d_{pw}, d_{pn}, d_z$ | Diffusion coefficients (in $\text{min}^{-1}$) |

way of scaling a system like this, and the scaling we have chosen is given in Table 1. With this scaling, our original equations take the somewhat simpler form (Tables 2, 3)

$$\frac{dmb}{dt} = \gamma_{mb}\{[(G_{BW}(pCt) + G_{BO}(po))F_{BB}(pb)]_{\tau_{mb}} - mb\} \tag{8}$$

$$\frac{dpb}{dt} = \gamma_{pb}(mb_{\tau_{pb}} - pb) \tag{9}$$

$$\frac{dmw}{dt} = \gamma_{mw}\{[G_{WB}(pb) + G_{WW}(pCt)]_{\tau_{mw}} - mw\} \tag{10}$$

$$\frac{\partial pw}{\partial t} = \gamma_{pw}(mw_{\tau_{pw}} - pw) + d_{pw}\frac{\partial^2 pw}{\partial x^2} \tag{11}$$

$$\frac{dpc}{dt} = \gamma_{pc}(G_{WC}(pw) - pc) \tag{12}$$

$$pct = K_{eq} \cdot pc \cdot tcf. \tag{13}$$

### 2.4 Parameter estimation

Even with the reduction in parameter numbers with the scaling we have chosen, the number remaining to be estimated is large. The values that we have used in our simulations are tabulated in Table 5 and their estimation is discussed in Appendix A. When we were unable to find reliable sources to estimate given parameters (e.g. kinetic constants and Hill coefficients) we elected to explore the corresponding parameter space to look at the numerical behavior of the model, and then examined the dependence of the results on these parameters through a sensitivity analysis (cf. Sect. 3.3).

## 3 Numerical results

The numerical calculations reported in Sect. 3 here have been carried out by solving the dynamical equations using XPPAUT. In examining the temporal dynamics we used a fourth order Runge Kutta integration scheme with a time step of $\Delta t = 0.025$. For the spatiotemporal computations we used a forward Euler method with space step of of $\Delta x = 0.1$ and $\Delta t = 0.025$ for simulations in both one and two dimensions (grid size: $100 \times 100$ and zero flux boundary conditions).

### 3.1 Temporal evolution in the absence of diffusion

The temporal dynamics for the $wnt8$–$blimp1$ subsystem are determined by Eqs. 8–13. To guide our selection of parameters we determined what parameter values lead to sustained temporal oscillations in the constituents of the $wnt8$–$blimp1$ subsystem. The results are tabulated in Table 4 which lists the threshold values of the parameters above which Wnt8 and Blimp1 oscillate. This set of parameters defines the boundary between stable and unstable (oscillatory) steady states and characterizes the Hopf bifurcation boundary for the system. An important observation is that oscillatory behavior is possible only if the total delay (transcription plus translation) exceeds a critical threshold value. This issue of the delay inducing an instability in the system will be taken up subsequently. The case of when oscillations in the $wnt8$–$blimp1$ system are not important because of the existence of sustained oscillations in the experimental data on the developing sea urchin embryo, but rather because within the context of our model we need to know where the boundary for these oscillations is in parameter space. In Appendices B and C we have examined the local stability of the reduced system. If parameters are chosen at or very near to the boundary (in the stable region, with

**Table 4** Parameter values for which sustained oscillations may be observed in the *wnt8–blimp1* subsystem and therefore defines the Hopf boundary for the system

| | |
|---|---|
| $\tau_{mb} + \tau_{pb}$ | >9 min |
| $\gamma_{mb}$ | >0.01 $\text{min}^{-1}$ |
| $\gamma_{mw}$ | >0.001 $\text{min}^{-1}$ |
| $\gamma_{pb}$ | >0.01 $\text{min}^{-1}$ |
| $\gamma_{pw}$ | >0.001 $\text{min}^{-1}$ |
| $k_{bw}$ | 0.03–0.8 |
| $k_{bb}$ | 0.03–0.3 |
| $k_{wb}, k_{bw}, k_{pc}, k_{cw}, k_{bc}, k_{wc}$ | >0.01 |
| $n_{bb}$ | >2 |
| $n_{bw}, n_{wb}, n_{ww}, n_{cw}, n_{bc}, n_{wc}$ | >0 |

**Table 5** Parameter values used in the computations to produce Figs. 2, 3, 4 and 5

| | |
|---|---|
| $\tau_{mb}, \tau_{mw}$ | 25 min (Santillan and Mackey 2008) |
| $\tau_{pb}$ | 3 min (Rodriguez-Gonzalez et al. 2007) |
| $\tau_{pw}$ | 1 min (Rodriguez-Gonzalez et al. 2007) |
| $\gamma_{mb}, \gamma_{mw}$ | 0.1 $\text{min}^{-1}$ |
| $\gamma_{pb}, \gamma_{pw}, \gamma_{pc}$ | 0.01 $\text{min}^{-1}$ |
| $k_{bw}, k_{bb}, k_{wb}, k_{ww}\ k_{wc}, k_{bc}, k_{pc}$ | 0.1 |
| $k_{wc}$ | 0.01 |
| $n_{bw}, n_{wb}, n_{ww}, n_{cw}, n_{bc}, n_{wc}$ | 3 |
| $n_{bb}$ | 1.2 |

$1 < n_{bb} < 2$ and the rest of the parameters as in Table 5), strongly damped oscillations are observed (Fig. 2). That this corresponds to the single pulse of gene expression as observed experimentally (Materna et al. 2010) will be shown in the next section.

### 3.2 Spatiotemporal dynamics

Not unexpectedly, the model dynamics becomes richer when diffusion of protein Wnt8 is also taken into account. The experimental studies with the sea urchin embryo (Materna et al. 2010) suggest that the expression of the genes *wnt8* and *blimp1* is initiated at the central region of the embryo. Very soon the protein Wnt8 diffuses out to the next ring of cells and activates the circuit there, while when a large quantity of Blimp1 protein has accumulated at the center, auto-repression of this protein shuts down its own expression as well as of the Wnt8 in the same region. Consequently, following their initial expression in the centrally located SM territory, expression of these genes disappears from the SM and is then activated in the NSM. Again after some hours, it is shut off in the NSM and activated in the next outer ring of developing endoderm cells, producing an expanding torus-like pattern of gene expression.

To mimic these events we need to simulate the dynamical equations in both space and time. We did simulations in both one and two spatial dimensions and the results

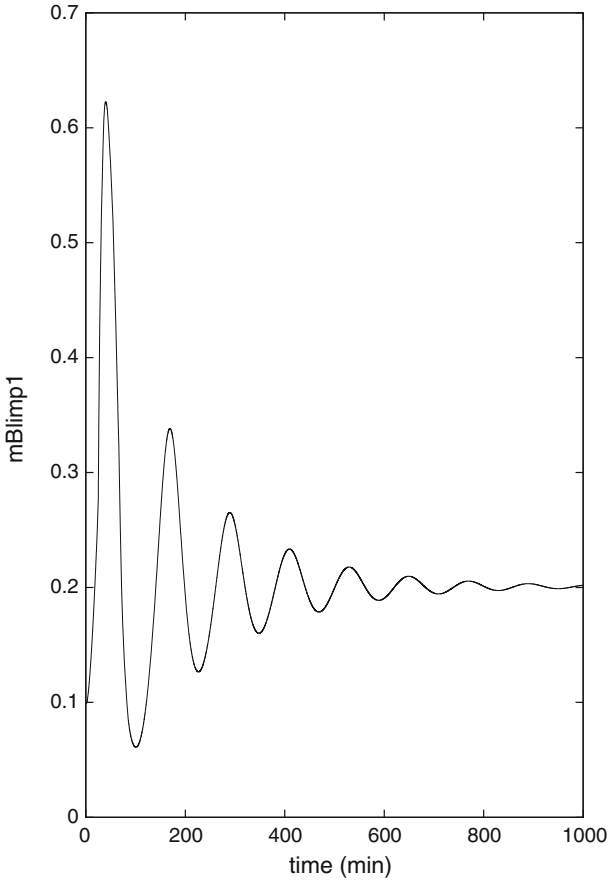


**Fig. 2** Results of simulation of the $wnt8$–$blimp1$ subsystem described by the set of Eqs. 8–13 (with the diffusion term in $pW$ dropped) using parameter values as given in Table 5

are presented in Figs. 3, 4 and 5. Ideally the diffusion coefficient should be taken from biochemical literature, as we have pointed out previously, but we have been unable to find reliable estimates so we used a scaled value of the order of $10^{-2}$ $\text{min}^{-1}$ for the diffusion coefficient of the protein Wnt8 (corresponding to an unscaled diffusion coefficient on the order of $10^{-8}$ $\text{cm}^2$ $\text{s}^{-1}$). Again we found that variation of this diffusion coefficient by even two orders of magnitude did not qualitatively alter the numerical results. Here it is of utmost importance to note that in the system that we are considering only Wnt8 protein has the capacity to diffuse.

We set zero initial values for all the concentration variables at all of the total 100 sites except near the center, at the space points 45–55 where we have started with values 0.1 for every variable. (Our results indicate that any arbitrary non-zero initial value gives the same result.) The choice of such an initial condition is motivated by the fact that maternally deposited mRNA and protein near the central region of the embryo initially breaks the symmetry of the system. In our simulation we found that

oscillations in concentrations of the protein and mRNA starting at this centrally located region soon propagate outward at a finite speed, corresponding to a traveling wave.

Figure 3 depicts the temporal evolution of $blimp1$ mRNA concentration at different spatial points while Fig. 4 illustrates the full spatiotemporal evolution of Blimp1 protein in one spatial dimension. Figure 5 shows the evolution pattern of Blimp1 in two dimensional space at different times.

To see how well our numerical simulation results match with the experimental behavior reference should be made to Figure 1 of Smith and Davidson (2008) which we reproduce in Fig. 6. Figure 6a schematically describes how the proteins (Blimp1 or Wnt8) start getting expressed at the center and then travel outwards. Figure 6c gives the expression of $wnt8$ and $blimp1$, visualized by WMISH. This can be nicely

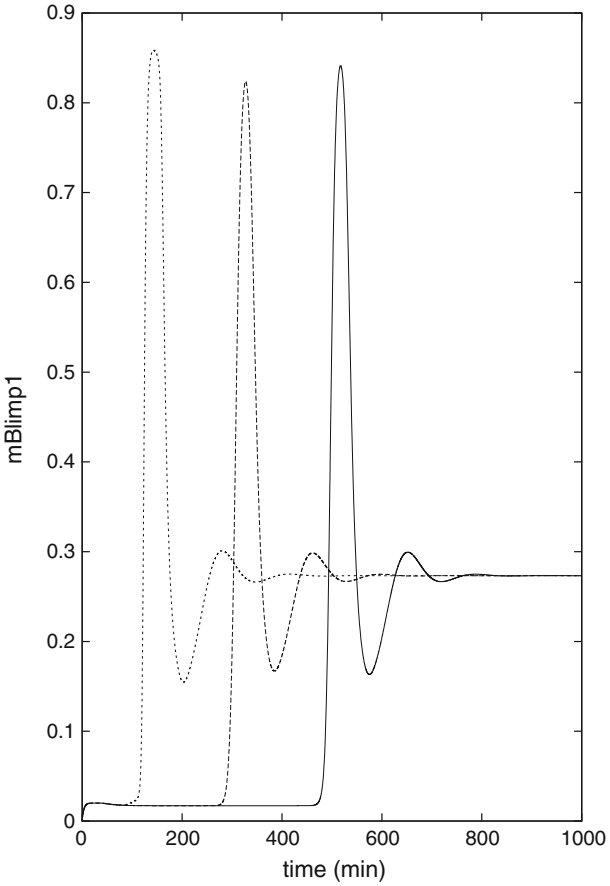


**Fig. 3** Results of simulation of the system described by the set of Eqs. 8–13 in extended space (in one dimension with a total number of spatial grids points = 100) using the model with the parameters given as in Table 5. The *solid*, *dashed* and the *dotted curves* represent the temporal evolution of $blimp1$ mRNA at spatial grid locations 40, 35 and 30 respectively. We took zero initial values for all the concentration variables at every site except near the center for space points 45–55. Along the axis we started with initial values 0.1 for every variable

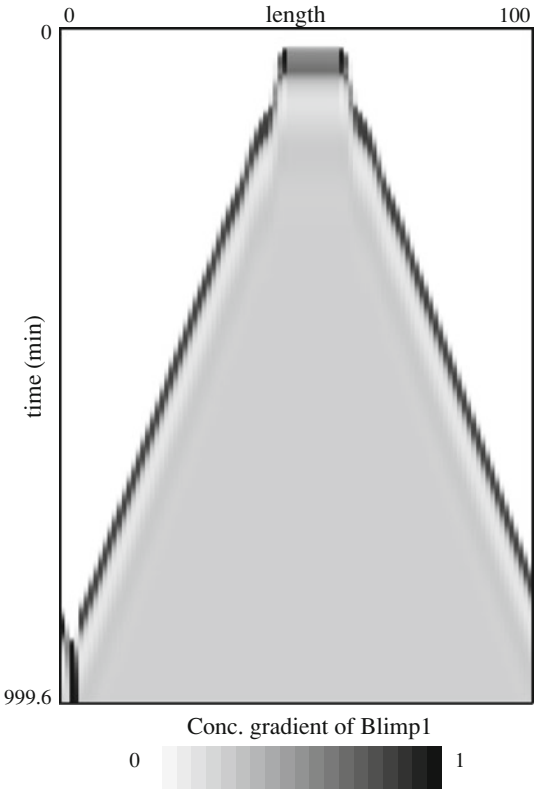


**Fig. 4** The spatiotemporal evolution of Blimp1 obtained by simulating the system given by the set of Eqs. 8–13 in extended space (in one dimension with a total number of spatial grids points =100) using the model with the parameters given as in Table 5. Initial conditions as in Fig. 3

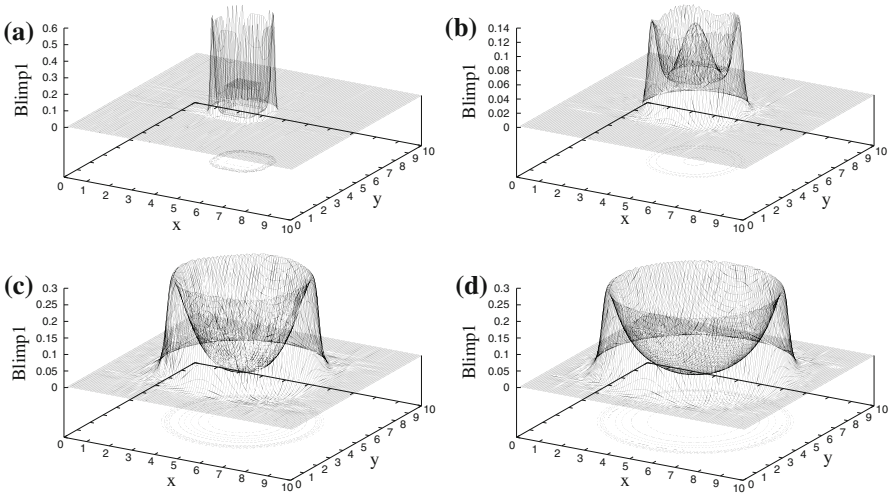


**Fig. 5** The spatiotemporal evolution of Blimp1 obtained by simulating the full system given by Eqs. 8–13 in two dimensional space with 100 × 100 grid points and parameter values in Table 5 at **a** 10 min, **b** 30 min, **c** 50 min, **d** 70 min. Initial conditions as in Fig. 3

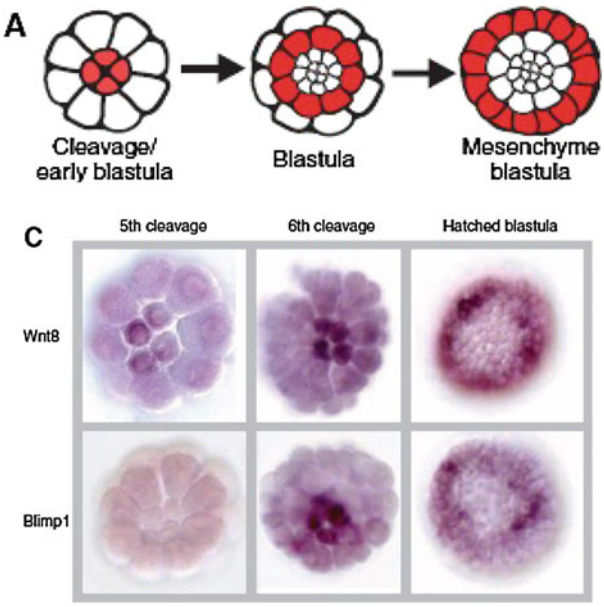


**Fig. 6** These two diagrams are reproduced from figure 1 of Smith and Davidson (2008). **a** schematically describes how the proteins (Blimp1 or Wnt8) start being expressed at the *center* and then travel *outwards.* **c** Gives the expression of *wnt*8 and *blimp*1, visualized by WMISH. This can be easily compared with the expression pattern predicted by the model here (cf. the contour in Figs. 5 or 11)

compared with the expression pattern predicted by the model here (cf. the contours in Figs. 5 or 11). The correspondence between the experimental data and the behavior of the model is evident.

The dimensionless velocity of the wave pulses has been numerically determined to be about $2.5 \times 10^{-2}$ min$^{-1}$ which corresponds to an actual velocity of $2.5 \times 10^{-3}$ mm min$^{-1}$. Since the total length of an embryo is of the order several 100 micrometers (Marzinelli et al. 2008) then the estimated time taken for the waves to propagate between various regions of the embryo would be of the order of a few hours which is comparable to that observed experimentally. Thus, in spite of the striking simplicity of the model the agreement with the experimental observations is good.

### 3.3 Parameter sensitivity of the model

For parameters like degradation rates of mRNAs or proteins or the Hill exponents, we have had to satisfy ourselves with estimating their approximate values by comparing with experimental data available for similar systems. Whether the results depend sensitively on these parameters should therefore be checked. Also the dependence of the oscillation properties with respect to the different parameters can give us an idea about the relative importance of various feedback loops in generating the basic instability.

We have examined how the amplitude and period of the oscillation vary with the parameters in a region where the decaying oscillation occurs at the four variables.

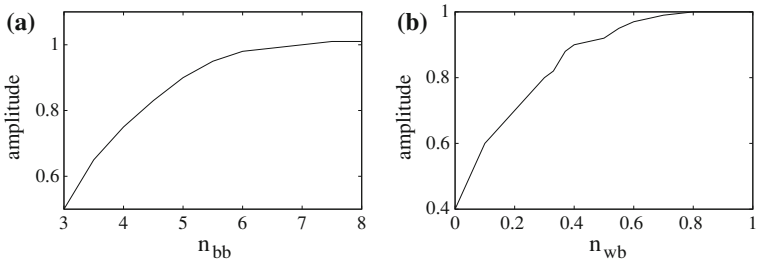


**Fig. 7** The variation of the oscillation amplitude solving the simplified set of Eqs. 30 in variables: **a** $mb$ versus $n_{bb}$, **b** $mb$ versus $n_{wb}$. All other parameters except the one that is varied have values given by Table 5

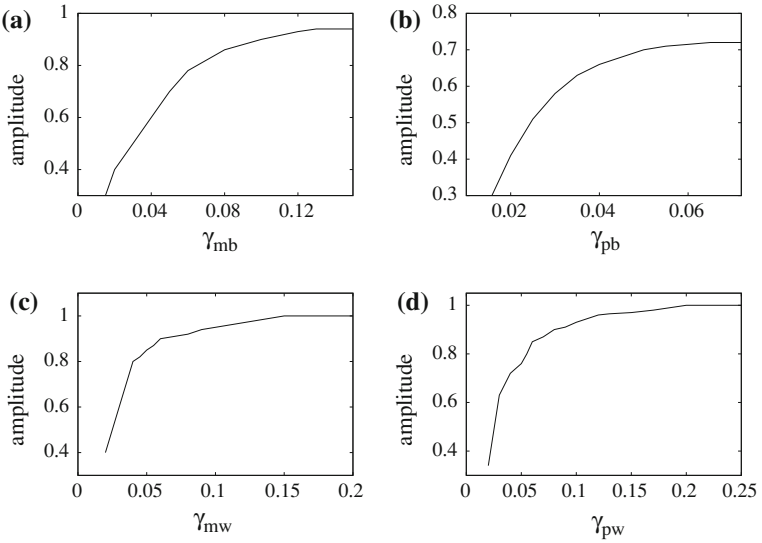


**Fig. 8** The variation of the amplitude of oscillation obtained from the simulation of Eq. 30 measured in the variables: **a** $mb$, **b** $pb$, **c** $mw$, **d** $pW$ respectively against their respective degradation rates. All other parameters except the one that has been varied have values given in Table 5

The variation of the amplitudes of the oscillations against the Hill coefficients is shown in Fig. 7. It should be borne in the mind at this juncture that the oscillatory behavior that we discuss here is transient in nature so amplitude or period may be assigned to the system only at the initial phase. For uniformity we take the height of the first peak as a measure of the amplitude and the distance between two successive peaks (of course they are of dissimilar lengths) as that of the period. In general amplitude increases with the Hill coefficient until it saturates at a value close to 1. However the variation is most sensitive to changes in $n_{bb}$. $n_{ww}$ has no observable effect on the amplitudes of any of the variables. Also we have found that none of these Hill coefficients influence the period of oscillation in any significant way.

The effect of the degradation rates on the amplitude of oscillation is shown in Fig. 8. The amplitude of a given variable increases and finally saturates as the degradation

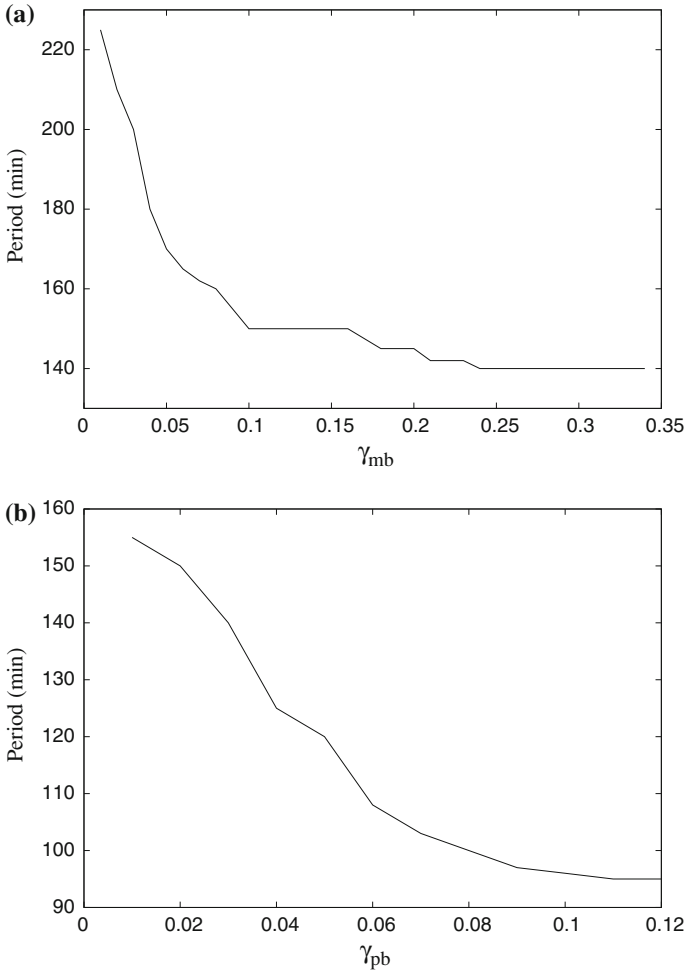


**Fig. 9** The variation of the oscillation period obtained from the simulations of the Eq. 30 (measured for the variable $blimp1$ mRNA) versus the degradation rates: **a** $\gamma_{mb}$, **b** $\gamma_{pb}$. All other parameters except the one that is varied have values given in Table 5

rate of the corresponding variable increases. The degradation rate of $blimp1$ mRNA and Blimp1 protein also affects the period of oscillation in lowering it to a limiting value as shown in Fig. 9. As expected this effect on the period is not observed in the case of the degradation rates corresponding to the other two variables.

We note the transient oscillatory behavior (which is essential for the generation of single pulse wave akin to the single pulse of gene expression that is observed experimentally in the sea urchin embryo) takes place for all the variables only if $n_{bb}$ is above 1, with all the other exponents having any value whatsoever. Even if we eliminate all other feedback loops except the auto-inhibitory one on mBlimp1, we still obtain damped oscillations in the variables $mb$ and $pb$ for $n_{bb} \geq 1$. (The oscillations are sustained at above $n_{bb} > 2$, but since this leads to a continuous generation of

traveling waves which is not relevant to the real biological observation it is outside the scope of this paper). This suggests that the coupled $blimp1$ mRNA-Blimp1 protein loop may oscillate autonomously and also that the auto inhibitory feed back loop due to Blimp1 protein on the transcription of corresponding mRNA is crucial in generating the instability. This $mb–pb$ oscillation then entrains the $wnt8$ mRNA-Wnt protein system at the $mb–pb$ frequency when the mRNA-Wnt protein system is coupled with it through a positive feedback loop involving the Blimp1 protein and $wnt8$ mRNA (this is obvious since a non zero value of the coefficient $n_{wb}$ is sufficient for the $mw$, $pw$ to oscillate as long as $n_{bb}$ stays above 1). This model prediction is in accord with earlier experimental results, but one recently published paper (Peter and Davidson 2011) contradicts this, claiming:

"Our results exclude an earlier model (23) proposing that clearance of blimp1b expression from the mesodermal domain, is responsible for clearance of wnt8 expression from this domain, on the assumption that Blimp1 is a necessary driver of wnt8 expression. This could ultimately lead to the down regulation of most endodermal regulatory genes, by removal of the Tcf/$\beta$-catenin signal that activates them. However, although mutation of Blimp1-binding sites reduces the activity of a small wnt8 cis-regulatory con- struct18, the same mutation does not affect expression of a bacterial artificial chromosome expression construct containing the whole genomic wnt8 cis-regulatory system (Supplementary Fig. 7). In any case, the expression of Wnt8 begins in veg2-derived cells long before the onset of blimp1b expression in these cells."

This observation thus suggests that $wnt8$ expression is independent of the protein Blimp1. But with our original model the exact expression profile of Wnt8 is seen to critically depend upon the Blimp1 negative feedback loop. This leads us to wonder whether some other kind of feedback loop may be present that enables Wnt8 to sustain its own evolution even without the presence of Blimp1. Also to correspond to the experimental situation of a single pulse of gene expression (Materna et al. 2010) the parameters have to be chosen at or very near to the boundary (in the stable region, with $1 < n_{bb} < 2$ and the rest of the parameters as in Table 5). Such stringent conditions on the parameters can be taken as a potential indication that our original hypothesis must be missing something. On this premise we offer a variation of the above model.

## 4 Modification of the model

As mentioned earlier we have to modify the above model based on the assumption that there is an additional feedback loop involving one of the proteins. This hypothesis is inspired by analogy of the spatial expression profile during embryogenesis of sea urchin with pattern formation during Hypostome, tentacle and foot formation in hydra.

At this point a few words on the pattern forming mechanism in hydra are appropriate. A recent model proposed by Meinhardt (2012) reproduces the positional information scheme required for the generation of head, tentacle and foot of hydra by a set of hierarchically coupled pattern forming systems. According to this scheme a structure generates the precondition of a second structure in the immediate neighborhood but excludes the second structure locally. The mechanism for pattern formation in the var-

ious regions (head, foot and tentacles) are determined by separate activator–inhibitor systems coupled together by a source density. The formation of this source density is activated by the head activator, in turn, the source density activates the head activator production. The foot activator has the opposite effect in that it inhibits source density production while the source density suppresses its own transcription. The head and the foot activators grow in different regions of space excluding the other one locally and themselves in the neighborhood. However, unlike hydra, the sea urchin system is not known to involve a diffusing inhibitor. The only diffusible protein present here is Wnt8 which acts as activator, which excludes the possibility of any kind of Turing-like structure formation. However there is some recent evidence suggesting Wnt8 may act as inhibitor in many systems similar to the sea urchin embryo. Meinhardt (2012), based on very recent observations, proposes a mechanism which suggests that Wnt molecules are re-processed from a slowly lipid-binding variety to a variety bound to small lipid particles that diffuse more rapidly. It is not yet known whether the differently processed Wnt's have different functions. The proposal is that the slow Wnt's act as activators and obtain inhibitory functions after the re-processing. Based on these observations we offer a modification of our modeling and then investigate whether or not the new model predictions tally with the experimental results. We assume that Wnt8 undergoes a reaction of (currently) unknown type which produces a species that inhibits Wnt8 production from the corresponding mRNA. The set of model equations would then look like

$$\frac{dmb}{dt} = \gamma_{mb}\{[(G_{bw}\,(pw) + G_{bo}\,(po))F_{bb}\,(pb)] - mb\} \tag{14}$$

$$\frac{dpb}{dt} = \gamma_{pb}(mb - pb) \tag{15}$$

$$\frac{dmw}{dt} = \gamma_{mw}\{[G_{wb}\,(pb) + G_{ww}\,(pw)]F_{wz}(z) - mw\} \tag{16}$$

$$\frac{\partial pw}{\partial t} = \gamma_{pw}(mw - pw) + d_{pw}\frac{\partial^2 pw}{\partial x^2} \tag{17}$$

$$\frac{dz}{dt} = \gamma_z(pw^2 - z) + d_z\frac{\partial^2 z}{\partial x^2} \tag{18}$$

Here $z$ is the hypothetical intermediate that Wnt8 produces through the unknown reaction and which diffuses at a rate faster than Wnt8 (Meinhardt 2012). The rate of its formation is enhanced due to Wnt8 and it has a natural first-order decay. This modified Wnt8 now inhibits the transcription of mWnt8. Thus we assume an inhibiting role of the diffusible protein Wnt8 (the new network circuitry now contains an additional negative self inhibition loop as shown in Fig. 10). Now, the model involves short range activation versus long range diffusion, a necessary precondition for a Turing mechanism to be operative. This dramatically alters the results.

The results of the simulation with Eqs. 14–18 are given in Fig. 11. (The simulations are performed by simple Euler finite difference technique in a $100 \times 100$ grid size with a time step of 0.001 and space interval of 1, boundary condition zero flux). The expanding ring like pattern is similar in nature to the one obtained with the former model, but as discussed above there are basic differences which we elaborate below.

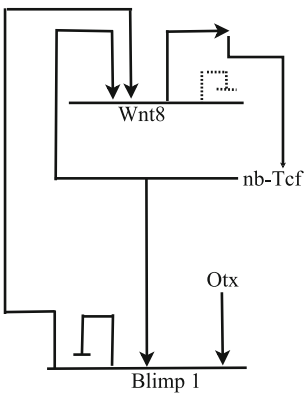


**Fig. 10** The gene regulatory network corresponding to the *wnt*8–*blimp*1 sub circuit with the additional negative feedback loop (shown in *dotted line*) which that we have proposed. The *lines* with *arrowheads* denote activation and the ones with *bluntheads* denote inhibition

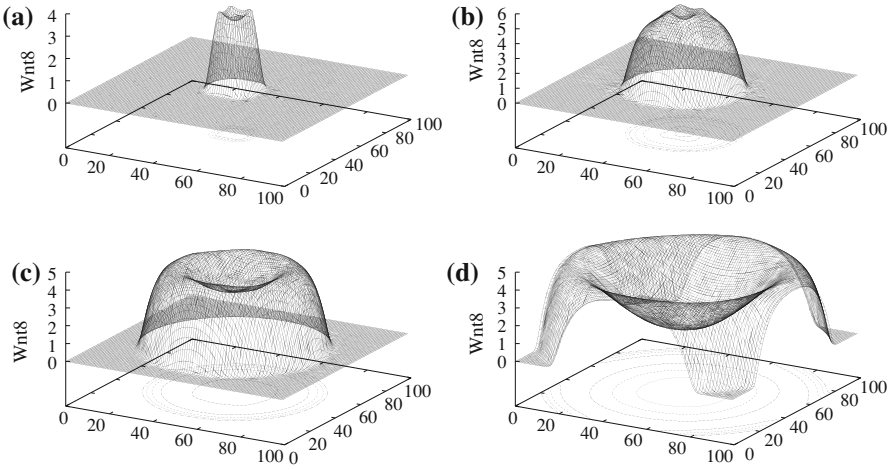


**Fig. 11** The spatiotemporal evolution of Wnt8 protein obtained by simulating the system given by Eqs. 14–18 in two dimensional space and parameter values as given in Table 6 with $100 \times 100$ grid points at **a** 5, **b** 10, **c** 15, **d** 20 min respectively. Initial conditions as in Fig. 3

**Table 6** Parameter values used in the computations to produce Fig. 11

| | |
|---|---|
| $\gamma_{mb}, \gamma_{mw}, \gamma_z$ | 0.1 $\text{min}^{-1}$ |
| $\gamma_{pb}, \gamma_{pw}$ | 0.01 $\text{min}^{-1}$ |
| $k_{bw}, k_{bb}, k_{ww}, k_{wz}$ | 0.1 |
| $k_{wb}$ | 1.0 |
| $n_{wz}, n_{ww}, n_{wb}, n_{cw}, n_{bc}, n_{wc}$ | 2 |
| $n_{bb}, n_{bw}$ | 1 |
| $d_{pw}$ | 0.5 $\text{min}^{-1}$ |
| $d_z$ | 1.0 $\text{min}^{-1}$ |

1. With the model of Sect. 2 the protein progression starts only once there is a Hopf bifurcation and therefore can be interpreted as the propagation of a traveling wave. In the modified version protein progression starts before such a bifurcation has

taken place and so must be looked at from a different point of view. Initiation of expression at the central part is due to an activating feedback from Wnt8, but soon the activating influence of Wnt8 is overcome by the inhibiting role of the same protein and therefore the structure becomes locally suppressed. But now Wnt8 has already diffused out to the next layer creating a condition of similar evolution at this next higher ring. Thus here too, like in hydra, a structure generates the precondition for another in the immediate neighborhood but excludes the structure locally.

2. We checked that even if we eliminate all transcriptional and translational delays and take the system away from the Hopf bifurcation region the ring like pattern still appears above the threshold values of each of the two Hill coefficients of the two feedback loops, one positive and the other negative due to Wnt8. With the previous model the expanding ring appears only within the Hopf region. Near the bifurcation boundary it is possible to obtain only one cycle of such a pattern, but if one goes deep into the region past the Hopf bifurcation the pattern repeats itself and this contradicts experimental observation of single pulse of gene expression. Therefore, as we earlier mentioned, the experimental parameters must remain close to the bifurcation boundary. At this point therefore the modified version has the edge over the original in being much more robust to parameter changes.
3. Here we note that the patterned structure critically depends only upon two of the many feedback loops: the activating and inhibitory ones, due to Wnt8, on its own formation. We noted the corresponding two Hill coefficients $n_{wz}$ and $n_{ww}$ have to be greater than 1.5 and 1.8 respectively. If either of these two loops are removed the pattern never appears. This is in contrast to the original model in which the key step was the negative feedback loop due to Blimp1 on $blimp1$ transcription. But as we have emphasized before a recently published paper rejects an earlier claim by the same group regarding the quintessential role of Blimp1 protein in the evolution of Wnt8. With the inclusion of the Wnt8 negative feedback in the model now the expression of *wnt8* is seen to be entirely independent of Blimp1, since the feedback loops due to Wnt8 can alone bring about the entire sequence of protein expressions and their observed spatial profile.

In the case of Hydra, one pattern forming system that is initially present becomes inhibited by a second one that dominates and displaces the first into an adjacent position. Therefore there is a shift, but no oscillations. The displacement of the signal is actually determined by the concentration of the source density (the source density concentration being a function of head activator concentration was actually breaking the over all symmetry of the system). In the case of the sea urchin a similar shift is brought about by the indirect inhibitory influence of Wnt8 through the hypothetical intermediate $z$.

However the role that Wnt8 plays here in this mechanism may also be played by some other diffusing inhibitor present in the system. A very recent investigation (Sethi et al. 2012) claims that Notch, which is known to have an inhibitory influence on the transcription of Wnt8, plays crucial role in the removal of Wnt8 during endo-mesodermal specification. Numerically we explored this possibility by replacing the dynamics of hypothetical 'z' with that of Notch. The dynamical system is then given as

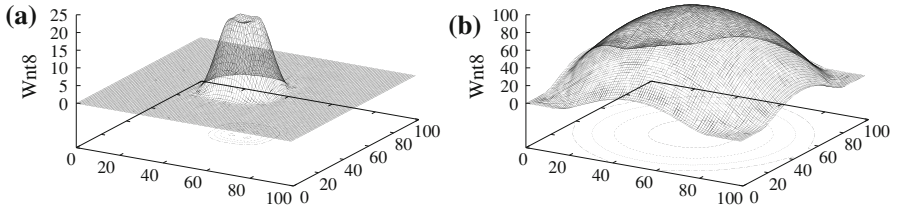


**Fig. 12** The spatiotemporal evolution of Wnt8 protein obtained by simulating the system given by Eqs. 19–24 in two dimensional space and parameter values as given in Table 7 with $100 \times 100$ grid points at **a** 10, **b** 40 min respectively. Initial conditions as in Fig. 3

**Table 7** Parameter values used in the computations to produce Fig. 12

| | |
|---|---|
| $\gamma_{mb}, \gamma_{mw}, \gamma_{mn}, \gamma_{pn}$ | $0.1\text{min}^{-1}$ |
| $\gamma_{pb}, \gamma_{pw}$ | $0.1\ \text{min}^{-1}$ |
| $k_{bw}, k_{bb}, k_{ww}, k_{wn}$ | 0.1 |
| $k_{wb}$ | 1.0 |
| $n_{wn}, n_{ww}, n_{wb}, n_{cw}, n_{bc}, n_{wc}$ | 2 |
| $n_{bb}, n_{bw}$ | 1 |
| $d_{pw}$ | $0.5\ \text{min}^{-1}$ |
| $d_n$ | $1.0\ \text{min}^{-1}$ |

$$\frac{dmb}{dt} = \gamma_{mb}\{[(G_{bw}\,(pw) + G_{bo}\,(po))F_{bb}\,(pb)] - mb\} \tag{19}$$

$$\frac{dpb}{dt} = \gamma_{pb}(mb - pb) \tag{20}$$

$$\frac{dmw}{dt} = \gamma_{mw}\{[G_{wb}\,(pb) + G_{ww}\,(pw)]F_{wz}(z) - mw\} \tag{21}$$

$$\frac{\partial pw}{\partial t} = \gamma_{pw}(mw - pw) + d_{pw}\frac{\partial^2 pw}{\partial x^2} \tag{22}$$

$$\frac{dmn}{dt} = \gamma_{mn}(F_{nu}(pu)G_{nb}(pb) - mn) \tag{23}$$

$$\frac{dpn}{dt} = \gamma_{pn}(mn - pn) + d_{pn}\frac{\partial^2 pn}{\partial x^2} \tag{24}$$

(The production term reflects activation via ubiquitously present Unk and repression mediated through protein Blimp1 (Davidson 2006)).

As can be seen from the simulation results (Fig. 12) once again there is a strong qualitative agreement with the experimental situation. Further it can be checked that the positive and the negative feedback loops on Wnt8, due to Wnt8 itself and the Notch protein (below a value of 0.8 for both the coefficient $n_{ww}$ and $n_{wn}$ the progression pattern vanishes) respectively are sufficient to bring about the entire sequence of gene expressions.

## 5 Discussion and concluding remarks

The gene-regulatory network of the developing sea-urchin embryo provides a rare opportunity to study the spatio-temporal progression of signaling waves. In this developmental system, the expression of the gene *blimp1* starts at the center and then move outwards in the form of a traveling wave front. In three dimensions this would give rise to an expanding torus-like pattern.

Next we introduced a negative feedback loop (due to Wnt8 protein) to the model noting a similar effect is present in some similar models. This dramatically alters the consequences. The phenomena of shifting of expression center now takes place even in the non-Hopf region suggesting that the occurrence could be interpreted in terms of local structure formation and its consequent effect on the immediate neighborhood. Though the feedback loop is not yet known to exist in sea urchin, its presence in other similar systems gives strong reasons to believe it to be present here as well. Furthermore,

1. The modification renders the system more robust in terms of parameter values. The parameter space where the phenomenon occurs need no longer be confined along the Hopf boundary. The only criteria now is that the Hill coefficient of any of the two loops (the negative or the positive one, involving wnt8 on its own transcription) has to be above a threshold value.
2. Though not demonstrated to date in the case of the sea urchin, the fact that Wnt8 may inhibit its own production has been demonstrated in many similar systems (Meinhardt 2012)
3. As mentioned earlier in a recently published paper Peter and Davidson (2011) withdraw their earlier claim that the clearance of $blimp1b$ expression from the mesodermal domain is responsible for clearance of $wnt8$ expression from this domain, noting that though mutation of Blimp1-binding sites lowers the activity of a small $wnt8$ cis-regulatory construct18, the same mutation could not affect expression of a bacterial artificial chromosome expression construct containing the whole genomic $wnt8$ cis-regulatory system. Also the expression of $wnt8$ starts in veg2-derived cells long before the initiation of $blimp1b$ expression in the cells. These observation suggests that Wnt8 expression could continue even in absence of $blimp1$. But with our original model the exact expression profile of $wnt8$ is seen to critically depend upon the Blimp1 negative feedback loop. However now with Wnt8 negative feedback included in the extended model it seems plausible that the expression of *wnt8* could be entirely independent of Blimp1, since the feedback loops due to Wnt8 can alone bring about the entire sequence of protein expressions and their observed spatial profile. Yet another recent publication suggests the possibility of the involvement of Notch in the clearance of Wnt8 from the mesodermal domain (Sethi et al. 2012). This possibility has been explored too as a variation of the more general model.

All these factors point toward the presence of a negative feedback loop on the transcription of $wnt8$. This may either involve part of Wnt8 protein itself or a Notch protein. However a more detailed experimental investigation along this line is required to ascertain whether such a feedback really exists and exactly which species it involves.

(If the role of Wnt8 is verified experimentally, this would definitely strengthen the hypothesis regarding the inhibiting effect of Wnt8 and may contribute to the elucidation of its exact mechanism and therefore has strong implications beyond just the sea urchin system.)

Finally it should be kept in mind that with time as the number of cells increases (due to cell division) the situation becomes more complex and the nature of the wave progression at these later stages of development may not follow the simple dynamical course as illustrated here. However at the initial stages we feel that this effect may be ignored and the model developed here may be used to study the origin and evolution of these traveling waves.

### 5.1 Specific model predictions

Starting with a general structure of a model that is based completely on existing GRN we suggested a modification to it aiming at explaining experimental results more faithfully. The modification predicts a completely different mechanism compared to the original one and with the current stage of experimental data available it is really difficult to ascertain which of the mechanisms is actually operative. However our inclination is towards the modified version for reasons which have been discussed earlier.

However there are implications from the model presented here that can be tested experimentally with the use of suitable mutants which might lead us to conclude which of the mechanism is operative.

1. If the $wnt8$ gene is silenced in a mutant species, the primitive model suggests that this should not hinder the pattern of expression of Blimp1 But according to the modified model this should lead to disappearance of the entire pattern of gene expression.
2. On the other hand if in a mutant the $blimp1$ gene is silenced the spatio-temporal patterns in both proteins Blimp1 and Wnt8 should be lost according to the initially proposed model but in case with the modified version this should not disturb the expression pattern of $Wnt8$.

**Acknowledgments** We thank Prof. Hans Meinhardt for extremely helpful discussion and suggestions, and for pointing out the experimental data that led to the second model of this paper. This work was supported by the Natural Sciences and Engineering Research Council (NSERC, Canada), the Mathematics of Information Technology and Complex Systems (MITACS, Canada), and the Alexander von Humboldt Stiftung. The work was carried out at McGill University,the University of Bremen and also at the Indian Association for the Cultivation of Science (India), who we both thank for their hospitality.

## Appendix A: Parameter estimation

Apart from the transcriptional and translational delays, three categories of parameters are involved in our model: the degradation rates, the kinetic rate constants and the Hill exponents.

- The length scale $l$ is taken to be $l = 0.1$ mm which corresponds to a diffusion coefficient on the order of $10^{-4}$ mm$^2$ min$^{-1}$. However as mentioned earlier vari-

ation even by a few orders of magnitude does not change the numerical results qualitatively. Since experimental studies (Smith et al. 2007) do not indicate any temporal or spatial variation in the concentrations of the ubiquitously present factors Otx, Unk, Ub and Runx, we take their concentrations to be constant. The Hill terms containing these factors then may be replaced by constant quantities, and we have used $G_{bo} = G_{hu} = G_{nu} = G_{dr} = 0.01$.

- Time delays due to transcription and RNA processing prior to translation are approximately estimated by adding the time it takes for the polymerase to transcribe a gene (with a speed of around 15–20 nucleotides per second) plus 4–5 min to account for the time elapsed between the completion of the splicing and the emergence of the matured RNA in the cytosol. Thus we took $\tau_{mb} = \tau_{mw} = 25$ min and $\tau_{mn} = \tau_{md} = \tau_{mh} = 15$ min for the transcriptional delays for these genes. Translational delays were calculated using a translation speed of 6 nucleotides per second. Therefore we compute $\tau_{pb} = 3$ min, $\tau_{pw} = 1$ min, and for the proteins we have used the values: $\tau_{pn} = \tau_{pd} = \tau_{ph} = 3$ min.
- Monk (2003), Giudicelli and Lewis (2004), Hirata et al. (2004) and Bernard et al. (2006) report half-lives for different proteins of the Hes family and their corresponding mRNA of about 25 min (which corresponds to a degradation rate of about 0.03 $\text{min}^{-1}$). We have taken similar degradation rates for the mRNAs corresponding to the genes that belong to the Notch signaling pathway, viz. *notch*, *hes*1 and *delta*: $\gamma_{mn} = \gamma_{md} = \gamma_{mh} = 0.03\ \text{min}^{-1}$
- Since generally proteins degrade more slowly than mRNA we have assumed $\gamma_{pn} = \gamma_{pd} = \gamma_{ph} = 0.003\ \text{min}^{-1}$ we were unable to find equivalent data for genes in the *wnt* signalling pathway and so we assumed $\gamma_{mw} = 0.1 = \gamma_{mb} = 0.1\ \text{min}^{-1}$. For the proteins we took $\gamma_{pw} = \gamma_{pb} = 0.01\ \text{min}^{-1}$. However we have checked that the results do not sensitively depend upon the value of degradation rates chosen. Increasing the degradation rates only increases the amplitude of oscillation until it reaches a limiting value as discussed in Sect. 3.3

We were unable to find reliable experimental sources to estimate the rest of the parameters, namely the kinetic constants and the Hill coefficients, so we decided to explore the model parameter space to ask what regions of parameter space host what types of dynamic behavior. We have discussed in detail in Sect. 3.3 how the variation in the Hill exponents affects the results.

## Appendix B: Stability analysis

Here we consider the stability of a homogeneous steady state of the reduced two variable system describing the *wnt*8–*blimp*1 system under the assumption that the corresponding mRNA are in a quasi steady state. Thus we are considering the system

$$\begin{aligned} \frac{dpb}{dt} &= \gamma_{pb}[(G_{BW}(pw_\tau) + G_{BO}(po))F_{BB}(pb_\tau) - pw] \\ \frac{\partial pw}{\partial t} &= \gamma_{pw}[G_{WW}(pw_\tau) + G_{WB}(pb_\tau) - pb] + d_{pw}\frac{\partial^2 pw}{\partial x^2}, \end{aligned} \tag{25}$$

again with $\tau = \tau_{mb} + \tau_{pb}$. Also we now replace $G_{BO}$ with some constant value, say $k$ as discussed earlier. The homogeneous steady state $(pb^*, pw^*)$ is given by the solution of these equations under the assumption that both temporal and spatial derivatives are zero, or explicitly by

$$\begin{aligned} 0 &= \gamma_{pb}[(G_{BW}(pw^*) + kF_{BB}(pb^*) - pw^*] \\ 0 &= \gamma_{pw}[G_{WW}(pw^*) + G_{WB}(pb^*) - pb^*]. \end{aligned} \tag{26}$$

Define deviations $u(x,t)$ and $v(x,t)$ from the homogeneous steady state by $u(x,t) = pb(x,t) - pb^*$ and $v(x,t) = pw(x,t) - pw^*$. Then, under the assumption that $u$, $v$ are both sufficiently small so we may linearize the system in the vicinity of $pf^*$, $pw^*$ the deviations $u$, $v$ will be given by the solutions of the pair of equations

$$\begin{aligned} \frac{du}{dt} &= \gamma_{pb}[F^{'*}_{BB}G^*_{WB}u_\tau + F^{'*}_{BB}ku_\tau - u + F^*_{BB}G^{'*}_{WB}v_\tau] \\ \frac{\partial v}{\partial t} &= \gamma_{pw}[G^{'*}_{WW}u_\tau + G^{'*}_{BW}v_\tau] - \gamma_{pw}v + d_{pw}\frac{\partial^2 v}{\partial X^2}. \end{aligned} \tag{27}$$

(Here we have used the notation $F^*$ to denote evaluation of the function $F$ at the steady state, while $F^{'*}$ is the partial derivative of $F$ (with respect to the argument) evaluated at the steady state.)

If we assume the spatiotemporal perturbations $u(x,t)$ and $v(x,t)$ have the form of traveling waves

$$u(t) = u_0 e^{x+\lambda t} \qquad \text{and} \qquad v(x,t) = v_0 e^{x+\lambda t}, \tag{28}$$

(in general $\lambda$ is a complex number) then substitution into the linearized equations 27 yields, after some algebra, the characteristic equation:

$$\lambda^2 + \beta_1\lambda + \beta_2 + [\beta_3\lambda + \beta_4]\exp(-\lambda * \tau) + \beta_5\exp(-2\lambda\tau) = 0 \tag{29}$$

wherein the coefficients $\beta_i$ are given by

$$\begin{aligned} \beta_1 &= \gamma_{pb} + \gamma_{pw} + d_{pw} \\ \beta_2 &= \gamma_{pb}(\gamma_{pw} + d_{pw}) + \gamma_{pw}(\gamma_{pw} + d_{pw})F^{'*}_{BB}G^*_{WW}G^{'*}_{BW} \\ &\quad -\gamma_{pb}(\gamma_{pw} + d_{pw})kF^{'*}_{BB}G^*_{BW} + (\gamma_{pw} + d_{pw})G^{'*}_{WW}F^*_{BB}G^{'*}_{BW} \\ \beta_3 &= -[\gamma_u F^{'*}_{BB}G^*_{WW} + (\gamma_{pw} + d_{pw})G^{'*}_{BW} + \gamma_{pB}kF^{'*}_{BB}] \\ \beta_4 &= -[\gamma_{pB}(\gamma_{pw} + d_{pw})G^*_{BW} + \gamma_{pb}(\gamma_{pw} + d_{pw})G^{'*}_{WB} \\ \beta_5 &= \gamma_{pb}\gamma_{pw}F^{'*}_{BB}G^*_{BW}G^{'*}_{WB} - \gamma_{pw}\gamma_{pb}kF^{'*}_{BB}G^*_{WB} + \gamma_{pw}G^{'*}_{WW}F^*_{BB}G^{'*}_{BW}. \end{aligned}$$

Positivity of the real part of $\lambda$ signals the appearance of an instability and once it becomes positive its magnitude can be taken as an approximate measure of the ensuing wave velocity.

## Appendix C: The *wnt*8–*blimp*1 system without diffusion

We first consider the temporal dynamics for the $wnt8$–$blimp1$ system in the absence of diffusion.

We observed numerically that sustained oscillations are observed only when the combined transcription plus translation delay of the $wnt8$–$blimp1$ system crosses a threshold value. The origin of the temporal instability that induces the oscillations can be traced to a delay induced supercritical Hopf bifurcation of the system (Adimy et al. 2006) as we outline in the remainder of this section. Very near to the Hopf bifurcation boundary strongly damped oscillations occurs, and it is then possible to generate a single pulse of gene expression in response to a transient central stimulus.

The six variable model describing the $blimp1$–$wnt8$ dynamics can be further simplified by dropping the dynamics of nuclearized $\beta$-$catenin$ or the complex $\beta$-$catenin$–$Tcsf$. The effect of the complex then could be incorporated in the model by replacing the term for complex with protein Wnt8. The system of Eqs. 8–13 (in the absence of diffusion) then becomes

$$\begin{aligned}
\frac{dmb}{dt} &= \gamma_{mb}([G_{BW}(pw_{\tau_m} + G_{BO}(pO))F_{BB}(pb_{\tau_m}) - mb]) \\
\frac{dpb}{dt} &= \gamma_{pb}[mb_{\tau_p} - pb] \\
\frac{dmw}{dt} &= \gamma_{mw}([G_{WW}(pw_{\tau_m}) + G_{WB}(pb_{\tau_m}) - mw] \\
\frac{dpw}{dt} &= \gamma_{pw}[mw_{\tau_p} - pw].
\end{aligned} \tag{30}$$

The numerical results obtained by solving this simpler system are equivalent to the original six dimensional model, and thus it is possible to obtain insight into the dynamics by considering this simpler version of the model.

To simplify further we assume the transcriptional and translational delays to be the same for both the components of the $wnt8$–$blimp1$ species and write $\tau_{mb} = \tau_{mw} = \tau_m$ and $\tau_{pb} = \tau_{pw} = \tau_p$. Because of their higher degradation rates (cf. Appendix A), $mw$ and $mb$ equilibrate rapidly compared to their corresponding proteins, so we may assume a quasi-steady state for $mw$ and $mb$ to obtain

$$\begin{aligned}
\frac{dpb}{dt} &= \gamma_{pb}[(G_{BW}(pw_\tau) + G_{BO}(O))F_{BB}(pb_\tau - pw], \\
\frac{dpw}{dt} &= \gamma_{pw}[G_{WW}(pw_\tau) + G_{WB}(pb_\tau) - pb],
\end{aligned} \tag{31}$$

wherein $\tau = \tau_m + \tau_p$.

As shown in Appendix B, linearization of Eq. 31 about their steady state values leads to a characteristic (eigenvalue) equation given by

$$\lambda^2 + b_1\lambda + b_2 + [b_3\lambda + b_4]e^{-\lambda\tau} + b_5e^{-2\lambda\tau} = 0 \tag{32}$$

The eigenvalue equation

$$\lambda^2 + b_1\lambda + b_2 + [b_3\lambda + b_4]e^{-\lambda\tau_a} + b_5 e^{-\lambda\tau_b} = 0 \tag{33}$$

has been studied for a system in which there are two different delays in the system (Adimy et al. 2006). It has been shown there that if

$$(b_2 + b_5)^2 - b_4^2 > 0 \quad \text{and} \tag{34}$$

$$(b_1^2 - 2(b_2 + b_5) - b_3^2) > 0 \tag{35}$$

are simultaneously satisfied, then the real part of the eigenvalue remains negative for any $\tau_a > 0$ if $\tau_b$ is zero. If both $\tau_a$ and $\tau_b$ are non-zero, as is the case here ($\tau = \tau_a$ and $2\tau = \tau_b$), above a threshold value of $\tau_b$ the system may lose its stability through a supercritical Hopf bifurcation.

The parameter range of Table 4 satisfies these conditions, and therefore since both the delay terms are non-zero (one is twice the other) we expect a delay-induced supercritical Hopf bifurcation as $\tau$ is increased ($2\tau$ crosses the required threshold).

Also it should be noted that the two delays (translational plus transcriptional) do not appear separately in the eigenvalue equation but rather as a sum. While numerically solving the original equations we found, as expected, that there is a threshold value of the sum of the two delays (around 9) above which sustained oscillations exist.

**Traveling wave behavior**

Our analysis with the original model based on experimentally observed interactions identifies the origin of the temporal instability in this system with the existence of a Hopf bifurcation, induced by a delay which is intrinsically present in the system due to translational and transcriptional time lags. On a spatial domain, at the Hopf bifurcation region, the instability results in the generation of traveling waves which originates at the center and sweeps outwards. Very near to the bifurcation boundary strongly damped oscillatory behavior is obtained on the spatial domain which has the signature as single pulse of wave similar to the experimentally observed single pulse of gene expression. Examples of delay-induced Hopf bifurcations leading to limit cycle oscillations are well known in biology. Thus, the role of delays is pivotal in generating the instabilities that are the hallmark of various periodic hematological disorders (Adimy et al. 2006; Foley and Mackey 2009). Transcriptional and translational delays play a central role in inducing the segmentation clock to generate oscillations that interact with the progressive chemical wave front to produce the somites (Rodriguez-Gonzalez et al. 2007; Santillan and Mackey 2008).

The uniqueness of the current study is that here the delay induces a Hopf bifurcation which finally imparts its signature on the extended space in generating pulses of expression activity that propagate spatially in time. Thus the phenomena can be looked upon as a delay induced generation of traveling waves. The role of delays in slowing down traveling wave fronts in reaction-diffusion systems has been demonstrated earlier

(Xingfu 2002). Also the existence of traveling wave solutions in connection with a population genetics model, with distributed delay kernel, at small average delay, has been reported (Guojian and Yuan 2006). In contrast to the later study we consider a fixed delay, and see that above a certain threshold value for the delays, when the system crosses a boundary in the multidimensional parameter space the system loses stability and exhibits limit cycle oscillations which finally gives rise to the generation of propagating wave pulses. On or very near to the bifurcation boundary strongly damped oscillations result and then it is possible to generate a single pulse of gene expression in response to a transient central stimulus, consistent with the experimental finding (Materna et al. 2010). This is the important situation to be considered for the sea urchin pattern of development. The velocity of the traveling wave can be calculated numerically by noting the distance a point on the wave, with a given phase, travels in a given time. The value can be then be compared with the real situation. In this section however we have computed the velocity approximately at a given temporal frequency using a linear analysis to check the consistency of our numerics.

As before we confine our considerations to the simplified version of the coupled $wnt8$–$blimp1$ system described by Eq. 30. Employing the quasi-steady state approximation used in Appendix B then leads us to consider the reduced two variable system of equations given by

$$\begin{aligned}\frac{dpb}{dt} &= \gamma_{pb}[(G_{BW}(pw_\tau) + G_{BO}(po))F_{BB}(pb_\tau) - pw(t)] \\ \frac{\partial pw}{\partial t} &= \gamma_{pw}[G_{WW}(pw_\tau) + G_{WB}(pb_\tau) - pb(t)] + d_{pw}\frac{\partial^2 pw}{\partial x^2},\end{aligned} \tag{36}$$

where, again, $\tau = \tau_{mb} + \tau_{pb}$. As we have shown in Appendix B, linearizing these two equations near the steady state $(pb^*, pw^*)$ and assuming the the deviation away from the steady state is of the form of a traveling wave with constant velocity $\lambda$ leads to an eigenvalue equation of form

$$\lambda^2 + \beta_1\lambda + \beta_2 + [\beta_3\lambda + \beta_4]\exp(-\lambda\tau) + \beta_5\exp(-2\lambda\tau) = 0. \tag{37}$$

Now in general $\lambda$ is a complex number so we write

$$\lambda = \lambda_R + i\omega, \qquad \lambda_R = \mathfrak{Re}\lambda,$$

to obtain an equation for $\lambda_R$

$$\begin{aligned}&\lambda_R^2 - \omega^2 + \beta_1\lambda_R + \beta_2 + [\beta_3\lambda_R + \beta_4]\exp(-\lambda_R\tau) \\ &\cos(\omega\tau) + \beta_5\cos(2\omega\tau)\exp(-2\lambda_R\tau) \\ &+\beta_3\omega\sin(\omega\tau)\exp(\lambda_R\tau) = 0.\end{aligned} \tag{38}$$

A positive value of $\lambda_R$ signals the presence of an instability and once $\lambda_R$ becomes positive its magnitude is an approximate measure of the velocity of the wave.

The eigenvalue equation is then iteratively solved for $\lambda_R$ for a given value of $\omega$. We found that at a value of $\omega \simeq 0.04$ min$^{-1}$ (calculated numerically) above a threshold

value of $\tau$ (at $\tau = 9$ min), $\lambda_R$ becomes positive. Interestingly, in our simulations the generation of a traveling wave front also starts at the same value of $\tau$ at which oscillations ensue in the absence of diffusion. The magnitude of the wave velocity calculated in the two cases however differs. For the parameter range in Table 5 the wave velocity calculated from the eigenvalue equation is about $2 \times 10^{-2}$ min$^{-1}$. In contrast the value found numerically for the same parameter values is around $6.0 \times 10^{-3}$ min$^{-1}$. Thus the agreement between the simulation results and the values predicted from the linearized system is qualitatively similar in spite of the approximations involved regarding the separation of time scales.

## References


Adimy M, Crauste F, Ruan S (2006) Periodic oscillations in leukopoiesis models with two delays. J Theor Biol 242:288

Bernard S, Cajavek B, Pujo-Menjouet L, Mackey MC, Herzel H (2006) Modeling transcriptional feedback loops: the role of Gro/TLE1 in hes1 oscillations. Philos Transact A Math Phys Eng Sci 364:1155–1170

Davidson EH (2002) A genomic regulatory network for development. Science 295:1669–1678

Davidson EH (2006) The regulatory genome: gene regulatory networks in development and evolution (academic, san diego). Academic Press, San Diego

Foley C, Mackey MC (2009) Dynamic hematological disease: a review. J Math Biol 58:285

Giudicelli F, Lewis J (2004) The vertebrate segmentation clock. Curr Opin Genet Dev 14:407–414

Guojian L, Yuan R (2006) Traveling waves for the population genetics model with delay. ANZIAM J 48:57–71

Hirata H, Bessho Y, Kokubu H, Masamizu Y, Yamada S, Lewis J, Kageyama R (2004) Instability of Hes7 protein is crucial for somite segmentation clock. Nat Genet 36:750–754

Livi CB, Davidson EH (2006) Expression and function of blimp1/krox, an alternatively tran-scribed regulatory gene of the sea urchin endomesoderm network. Dev Biol 293(2):513–525

Marzinelli EM, Penchaszadeh PE, Bigatti G (2008) Egg strain in the sea urchin *Pseudechinus magellanicus*. Rev Biol Trop 56:335

Materna SC, Nam J, Davidson EH (2010) High accuracy, high resolution prevalence measurement for the majority of locally expressed regulatory genes in early sea urchin development. Gene Expr Patterns 10:177–184

Meinhardt H (2012) A model for pattern formation of hypostome, tentacles and foot in hydra: how to form structures close to each other, how to form them at a distance. Dev Biol 157:321–333

Minokawa T, Wikramanayake AH, Davidson EH (2005) cis-regulatory inputs of the wnt8 gene in the sea urchin endomesoderm network. Dev Biol 288(2):545–558

Monk NAM (2003) Oscillatory expression of hes1, p53, and nf-kappab driven by transcriptional time delays. Curr. Biol. 13(16):1409–1413

Peter IS, Davidson EH (2011) A gene regulatory network controlling the embryonic specification of endoderm. Nature 474:635–639

Rodriguez-Gonzalez JG, Santillan M, Fowler AC, Mackey MC (2007) The segmentation clock in mice: interaction between the Wnt and Notch signalling pathways. J Theor Biol 248:37–47

Santillan M (2008) On the use of Hill functions in mathematical models of gene regulatory networks. Math Model Nat Phenom 3:85–97

Santillan M, Mackey MC (2008) A proposed mechanism for the interaction of the segmentation clock and the determination front in somitogenesis. PLoS ONE 3(2):e1561

Sethi AJ, Wikramanayake RM, Angerer RC, Angerer RCRLM (2012) Sequential signaling crosstalk regulates endomesoderm segregation in sea urchin embryos. Science 335:590–593

Smith J, Davidson EH (2008) Gene regulatory network sub-circuit controlling a dynamic spatial pattern of signalling in the sea urchin embryo. PNAS 105(51):20089

Smith J, Theodoris C, Davidson EH (2007) A gene regulatory network sub circuit drives a dynamic pattern of gene expression. Science 318:794–797

Xingfu Z (2002) Delay induced travelling wave fronts in reaction diffusion equations of kpp-fisher type. J Comput Appl Math 146(2):309